

We are IntechOpen, the world's leading publisher of Open Access books Built by scientists, for scientists

6,900

Open access books available

186,000

International authors and editors

200M

Downloads

Our authors are among the

154

Countries delivered to

TOP 1%

most cited scientists

12.2%

Contributors from top 500 universities



WEB OF SCIENCE™

Selection of our books indexed in the Book Citation Index
in Web of Science™ Core Collection (BKCI)

Interested in publishing with us?
Contact book.department@intechopen.com

Numbers displayed above are based on latest data collected.
For more information visit www.intechopen.com



Performance Analysis for NOMA Relaying System in Next-Generation Networks with RF Energy Harvesting

Dac-Binh Ha and Jai P. Agrawal

Abstract

In this chapter, we investigate the performance of the non-orthogonal multiple access (NOMA) relaying network with radio-frequency (RF) power transfer. Specifically, this considered system consists of one RF power supply station, one source, one energy-constrained relay, and multiple energy-constrained NOMA users. The better user and relay can help the source to forward the message to worse user by using the energy harvested from the power station. The triple-phase harvest-transmit-forward transmission protocol is proposed for this considered system. The exact closed-form expressions of outage probability and throughput for each link and whole system are derived by using the statistical characteristics of signal-to-noise ratio (SNR) and signal-to-interference-plus-noise ratio (SINR) of transmission links. In order to understand more detail about the behavior of this considered system, the numerical results are provided according to the system key parameters, such as the transmit power, number of users, time switching ratio, and power allocation coefficients. The simulation results are also provided to confirm the correctness of our analysis.

Keywords: outage probability, non-orthogonal multiple access, relaying, radio frequency, wireless energy harvesting

1. Introduction

Radio-frequency (RF) energy harvesting (EH), abbreviated as RF-EH, enabled wireless power transfer (WPT) is an emerging and promising approach to supply everlasting and cost-effective energy to low-power electronic devices, that is, sensor nodes, low-power cellphone, wireless control devices, and so on [1–3]. This approach is expected to have abundant applications in next-generation wireless networks, such as Internet-of-Things (IoT) wireless networks or 5G networks, which can be a platform for varied fields, for example, manufacturing [4, 5], smart agriculture [5], and smart city [5]. Specifically, the IoT-based wireless sensor networks for smart agriculture usually consist of a large number of battery-powered wireless sensor nodes for data collecting, data processing, and data transmission. Therefore, these energy-constrained devices need to be replaced or recharged periodically; this leads the lifetime of network limited. The RF energy harvesting

can prolong the lifetime of these networks using the energy harvested from the RF sources (e.g., base station, TV/radio broadcast station, microwave station, satellite earth station, etc.). Compared with other resources available for the EH, the RF power is easy to be converted. Therefore, RF energy harvesting is the solution to enhance the system energy efficiency in the energy-constrained networks, including network lifetime; reduction of carbon footprint, without requiring battery replacement; easy and fast deployment in complicated or toxic environments; etc. In the past few years, there have been a number of works on RF energy harvesting communications, and the main works focused on the development of energy harvesting models, protocols, transmission schemes, and security in communication systems [1–3]. In practice, RF-EH can be operated in a time switching (TS) scheme in which the receiver uses a portion of time duration for energy harvesting and the remaining time for information receiving or a power splitting (PS) scheme in which the received signal power is divided into two parts for energy harvesting and information receiving, separately [6].

Relaying communication technique can mitigate the wireless channel fading and improve the reliability of wireless links by exploiting the spatial diversity gains inherent in multiple user environments [7]. This can be achieved by using collaboration of relay nodes to form virtual multiple input multiple output (MIMO) without the need of multiple antennas at each node. **Figure 1** depicts a system model of cooperative network. We can observe from this figure that the destination D can receive two signals from direct link and relaying link. It means that D has more opportunities to decode its own message; thus the performance of this system can be improved. There are two schemes of relaying technique: amplify-and-forward (AF) or decode-and-forward (DF). In AF relaying scheme, the relay simply sends a scaled copy of the received noisy signal to the destination, while in DF relaying scheme, the relay transmits a re-encoded copy to the destination, if the relay can successfully decode the transmitted message. In wireless relaying networks (e.g., energy-constrained wireless sensor networks), the relay nodes (e.g., cluster head nodes) are often subject to space limitation to equip a large battery for long lifetime using [8]. Thus, RF energy harvesting technique has been applied for this type of relay nodes to not only improve the throughput and reliability by exploiting the virtual spatial diversity but also promise everlasting network lifetime without requiring battery replacement. Due to the new imposed time-varying energy constraints, several technical issues, such as relaying protocols, power allocation, energy-information tradeoff, relay selection, cooperative spectrum sensing and sharing, security, etc., have been investigated for various relaying network models [6, 9, 10]. The challenges in these works become more complicated because the

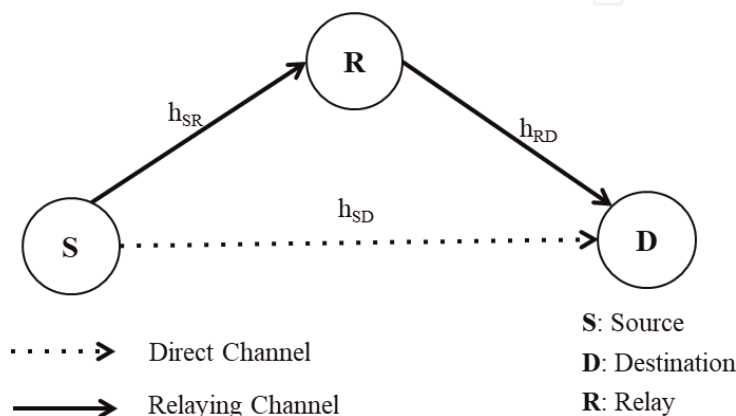


Figure 1.
A system model of cooperative network.

harvested energy varies according to channel fading, and the energy usage overtime needs to make a tradeoff between energy harvesting time and information processing time.

The next-generation networks (5G and beyond) are supported with very high data rate, ultralow latency, massive connections, and very high mobility to satisfy the fast-increasing users and demands. To fulfill these targets, the relaying and non-orthogonal multiple access (NOMA) techniques are proposed to extend the coverage of network, improve the performance, achieve high spectral efficiency, and support dense networks [11]. In NOMA scheme, the source superposes all messages before transmitting them to users as **Figure 2**. In this figure, we can see that the near receiver (or better user) uses successive interference cancelation (SIC) to obtain the far user's message first (due to it is allocated with more transmit power) and subtracts this component from the received signal to obtain its own message. Compared to conventional orthogonal multiple access (OMA), for example, frequency division multiple access (FDMA), time division multiple access (TDMA), and code division multiple access (CDMA), NOMA simultaneously serves multiple user equipment on the same resource blocks by splitting users into power domain [11]; therefore it can improve spectral efficiency of wireless network.

The above three techniques (i.e., RF-EH, relaying, NOMA) can be integrated into next-generation networks. However, there are many related issues that need to be addressed before these techniques can be deployed in next-generation networks, such as the network architecture, power allocation, relaying scheme selection, the combination between NOMA and other multiple access methods, fixed or dynamic user pairing/clustering, optimal user allocation and beamforming in NOMA MIMO systems, the impact of imperfect CSI, and joint optimization of diverse aspects of NOMA (spectrum efficiency, energy efficiency, security) [11]. In recent years, a number of works investigated some related issues such as performance of energy harvesting DF/AF relaying, cooperative, cognitive, and MIMO NOMA networks [12–15]. In addition, the work of [16] studied the secrecy performance of MIMO NOMA system over Nakagami- m channels with transmit antenna selection protocol. However, almost in these works the information sources are assumed that it can transmit RF energy and information by using TS or PS scheme.

Different from the above works, in this chapter we investigate the cooperative NOMA network in which the power station and information source (e.g., base station) are separated and the energy-constrained user nodes collaborate with the energy-constrained relay nodes to help source forward the information to destinations. The main contributions of this chapter are as follows:

- The triple-phase harvest-transmit-forward transmission protocol is proposed for this considered system.

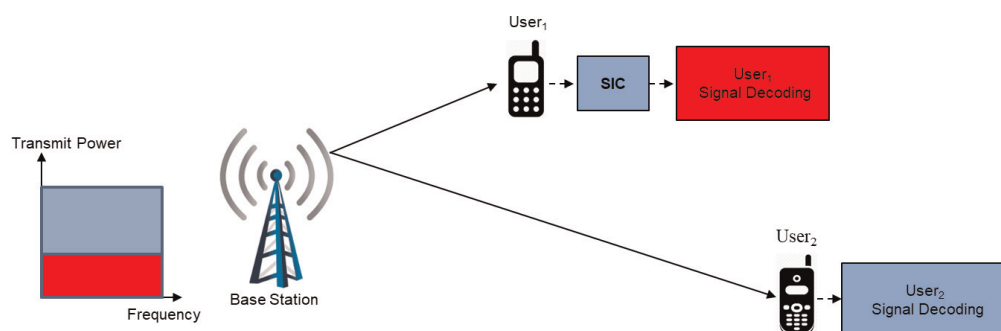


Figure 2.
Illustration of NOMA.

- The exact closed-form expressions of outage probability and throughput for each link and whole system are derived by using the statistical characteristics of signal-to-noise ratio (SNR) and signal-to-interference-plus-noise ratio (SINR) of transmission links.
- In terms of outage probability, the numerical results are provided according to the system key parameters, such as the transmit power, number of users, time switching ratio, and power allocation coefficients to look insight this considered system.

2. System and channel model description

Figure 3 depicts the system model for RF-EH NOMA relaying network, in which the power station (P) intends to transfer energy to energy-constrained relay (R) and energy-constrained destination nodes (D); information source (S) intends to transmit the information to destinations by the help of relay node R .

Notation: Denote P , S , R , and D as power station, information source, relay, and destination, respectively. $|h_{SDm}|^2$ and $|h_{SDn}|^2$ are denoted as the ordered channel gains of the m th user and the n th user, respectively. Denote $|h_{PR}|^2$, $|h_{PDm}|^2$, $|h_{SR}|^2$, $|h_{RDn}|^2$, and $|h_{mn}|^2$ as the channel gains of the links $P-R$, $P-D_m$, $S-R$, $R-D_n$, and D_m-D_n , respectively. Denote d_{PR} , d_{PDm} , d_{SR} , d_{RDn} , d_{SDm} , and d_{mn} as the Euclidean distances of $P-R$, $P-D_m$, $S-R$, $S-D_m$, $R-D_n$, and D_m-D_n , respectively. Symbol θ is denoted as the path loss exponent. Let $X_1 = |h_{PDm}|^2$, $Y_1 = |h_{PR}|^2$, $X_2 = |h_{SDm}|^2$, $Y_2 = |h_{SR}|^2$, $X_3 = |h_{mn}|^2$, and $Y_3 = |h_{RDn}|^2$.

In this system, NOMA scheme is applied for M destination users in pair division manner, such as $\{D_m, D_n\}$ with $m < n$ [17]. Without loss of generality, we assume that all the channel power gains between S and D_i ($1 \leq i \leq M$) follow the following order: $|h_{SD1}|^2 \geq \dots \geq |h_{SDm}|^2 \geq |h_{SDn}|^2 \geq \dots \geq |h_{SDM}|^2$.

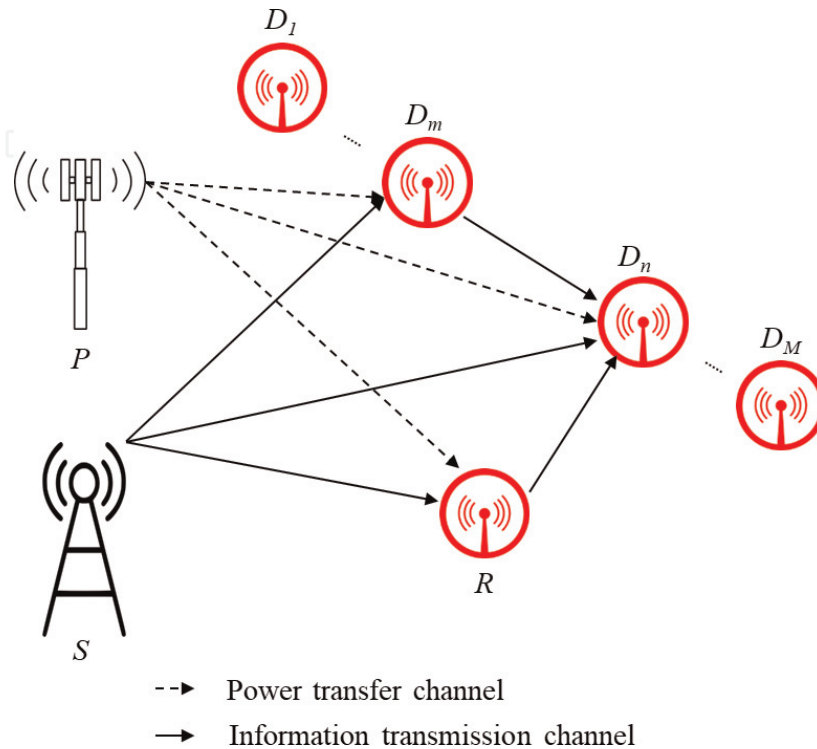


Figure 3.
System model for RF-EH NOMA relaying network.

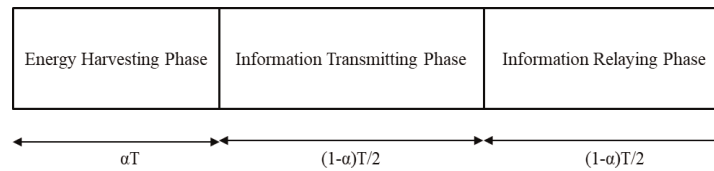


Figure 4.
 The triple-phase protocol for RF-EH NOMA relaying network.

The scenario of this considered system is investigated as follows:

- Due to the severe shadowing environment, the worse node (i.e., D_n) cannot detect message signal transmitted from S. Thus, the better node (i.e., D_m) or relay node R is selected to help S forwarding the message signal to worse node.
- All the transceivers are equipped by single antenna and operate in half duplex mode.
- All wireless links are assumed to undergo independent frequency nonselective Rayleigh block fading and additive white Gaussian noise (AWGN).
- The power gains of all links are modeled by random variables with zero mean and the same variance σ^2 , that is, $\sim CN(0, \sigma^2)$.

In this work, we propose a triple-phase harvest-transmit-forward transmission protocol for this RF-EH NOMA relaying system as shown in **Figure 4**:

1. In the first phase (power transfer phase): P transfers RF energy to the users with power P_0 in the time αT ($0 \leq \alpha \leq 1$, time switching ratio; T, block time for each transmission).
2. In the second phase (information transmitting phase): S uses power P_S to transmit superimposed message signal

$$x = \sqrt{a_m} s_m + \sqrt{a_n} s_n \quad (1)$$

to user pair (D_m, D_n) in the time of $(1-\alpha)T/2$, where s_m and s_n are the message for the m th user D_m and the n th user D_n , respectively, and a_m and a_n are the power allocation coefficients which satisfied the conditions: $0 < a_m < a_n$ and $a_m + a_n = 1$ by following the NOMA scheme. By applying NOMA, D_m uses SIC to detect message s_n and subtracts this component from the received signal to obtain its own message s_m .

3. In the third phase (information relaying phase): in this phase, D_m re-encodes and forwards s_n to D_n in the remaining time of $(1-\alpha)T/2$ with the energy harvested from P. At the same time, relay decodes x and forwards x to D_n .

Finally, D_n combines two received signals, that is, the relaying signals from D_m and R, to decode its own message by using selection combining (SC) scheme.

For more detailed purpose, we continue to present the transmission of this protocol for RF-EH NOMA relaying system in mathematical manner.

2.1 Power transfer phase

In this phase, the energy of D_m and R harvested from P in the time of αT can be respectively expressed as

$$E_1 = \frac{\eta P_0 |h_{PD_m}|^2 \alpha T}{d_{PD_m}^\theta}, \quad (2)$$

$$E_2 = \frac{\eta P_0 |h_{PR}|^2 \alpha T}{d_{PR}^\theta}, \quad (3)$$

where η is the energy conversion efficiency ($0 \leq \eta \leq 1$).

2.2 Information transmitting phase

In this duration of $(1-\alpha)T/2$, the source S broadcasts superimposed message signal x as Eq. (1) to the user pair and relay. The received signal at D_m is written as

$$y_{SD_m} = \sqrt{\frac{P_S}{d_{SD_m}^\theta}} (\sqrt{a_m} s_m + \sqrt{a_n} s_n) h_{SD_m} + n_{SD_m}, \quad (4)$$

where $n_{SD_m} \sim \text{CN}(0, \sigma^2)$ is AWGN.

Similarly, the received signal at R is expressed as

$$y_{SR} = \sqrt{\frac{P_S}{d_{SR}^\theta}} (\sqrt{a_m} s_m + \sqrt{a_n} s_n) h_{SR} + n_{SR}, \quad (5)$$

where $n_{SR} \sim \text{CN}(0, \sigma^2)$ are AWGN.

Applying NOMA, D_m uses SIC to detect message s_n and subtracts this component from the received signal to obtain its own message s_m . Therefore, the instantaneous SINR at D_m to detect s_m and s_n transmitted from S can be respectively given by

$$\gamma_{SD_m}^{s_n} = \frac{a_n \gamma_S |h_{SD_m}|^2}{a_m \gamma_S |h_{SD_m}|^2 + d_{SD_m}^\theta} = \frac{b_2 X_2}{b_1 X_2 + 1}, \quad (6)$$

$$\gamma_{SD_m}^{s_m} = \frac{a_m \gamma_S |h_{SD_m}|^2}{d_{SD_m}^\theta} = b_1 X_2, \quad (7)$$

$$\text{where } \gamma_S = \frac{P_S}{\sigma^2}, b_1 = \frac{a_m \gamma_S}{d_{SD_m}^\theta}, b_2 = \frac{a_n \gamma_S}{d_{SD_m}^\theta}.$$

And in the meanwhile the relay applying DF scheme first decodes its received signal from S to obtain superimposed message x and then re-encodes and forwards it to the destination. Therefore, in this phase the instantaneous SNR at R to detect x transmitted from S can be given by

$$\gamma_{SR}^x = \frac{\gamma_S |h_{SR}|^2}{d_{SR}^\theta} = b_3 Y_2, \quad (8)$$

$$\text{where } b_3 = \frac{\gamma_S}{d_{SR}^\theta}.$$

2.3 Information relaying phase

In this phase, D_m and R spend the harvested energy E_1 and E_2 , respectively, as Eqs. (2) and (3) to forward received signals to D_n in duration of $(1-\alpha)T/2$. Notice

that we ignore the processing power required by the transmit/receive circuitry of D_m and R . Therefore, the transmit power of D_m and R is respectively given by

$$P_1 = \frac{2\eta\alpha P_0 |h_{PD_m}|^2}{(1-\alpha)d_{PD_m}^\theta}, \quad (9)$$

$$P_2 = \frac{2\eta\alpha P_0 |h_{PR}|^2}{(1-\alpha)d_{PR}^\theta}. \quad (10)$$

The received signals at D_n that are transmitted from D_m and R are, respectively, expressed as

$$y_{D_m D_n} = \sqrt{\frac{P_1}{d_{mn}^\theta}} s_n h_{mn} + n_{mn}, \quad (11)$$

where $n_{mn} \sim \text{CN}(0, \sigma^2)$, and

$$y_{RD_n} = \sqrt{\frac{P_2}{d_{RD_n}^\theta}} (\sqrt{a_m} s_m + \sqrt{a_n} s_n) h_{RD_n} + n_{RD_n}, \quad (12)$$

where $n_{RD_n} \sim \text{CN}(0, \sigma^2)$.

Because D_n applies SC scheme, the instantaneous SNR/SINR at D_n to detect s_n transmitted from S can be given by

$$\begin{aligned} \gamma_{D_n}^{s_n} &= \max \left\{ \frac{2\eta\alpha\gamma_0 |h_{PD_m}|^2 |h_{mn}|^2}{(1-\alpha)d_{PD_m}^\theta d_{mn}^\theta}, \frac{2\eta\alpha a_n \gamma_0 |h_{PR}|^2 |h_{RD_n}|^2}{(1-\alpha)d_{PR}^\theta (a_m \gamma_0 |h_{RD_n}|^2 + d_{RD_n}^\theta)} \right\} \\ &= \max \left\{ c_1 X_1 X_3, \frac{c_2 Y_1 Y_3}{(c_3 Y_3 + 1)} \right\}, \end{aligned} \quad (13)$$

$$\text{where } \gamma_0 = \frac{P_0}{\sigma^2}, c_1 = \frac{2\eta\alpha\gamma_0}{(1-\alpha)d_{PD_m}^\theta d_{mn}^\theta}, c_2 = \frac{2\eta\alpha a_n \gamma_0}{(1-\alpha)d_{PR}^\theta d_{RD_n}^\theta}, c_3 = \frac{a_m \gamma_0}{d_{RD_n}^\theta}.$$

The independent and identically distributed (IID) Rayleigh channel gains ($X_1, Y_1, X_2, Y_2, X_3, Y_3$) follow exponential distributions with parameters $\lambda_1, \lambda_2, \lambda_3, \lambda_4, \lambda_5$, and λ_6 , respectively. According to [18], the cumulative distribution function (CDF) and the probability density function (PDF) of ordered random variable X_2 are respectively written as follows

$$F_{X_2}(x) = \frac{M!}{(M-m)!(m-1)!} \sum_{k=0}^{m-1} \frac{C_k^{m-1} (-1)^k}{M-m+k+1} \left[1 - e^{-\frac{x(M-m+k+1)}{\lambda_3}} \right], \quad (14)$$

$$f_{X_2}(x) = \frac{M!}{(M-m)!(m-1)! \lambda_3} \sum_{k=0}^{m-1} C_k^{m-1} (-1)^k e^{-\frac{x(M-m+k+1)}{\lambda_3}}. \quad (15)$$

Because all links undergo Rayleigh fading, the PDF and CDF of random variable $V \in \{X_1, Y_1, Y_2, X_3, Y_3\}$ have the following forms:

$$f_V(x) = \frac{1}{\lambda} e^{-\frac{x}{\lambda}}, \quad (16)$$

$$F_V(x) = 1 - e^{-\frac{x}{\lambda}}, \quad (17)$$

where $\lambda \in \{\lambda_1, \lambda_2, \lambda_4, \lambda_5, \lambda_6\}$.

3. Performance analysis

3.1 Outage probability

Outage probability is an important performance metric for system designers [12]. It is generally used to characterize a wireless communication system and defined as the probability that the instantaneous end-to-end SNR (γ_{e2e}) falls below the predetermined threshold γ_{th} ($\gamma_{th} = 2^{\Omega} - 1$, where Ω is fixed transmission rate at the source), given by

$$P_{out} = \Pr(\gamma_{e2e} < \gamma_{th}). \quad (18)$$

In this considered system, the outage event at the destination occurs when D_m cannot detect successfully s_n or s_m or when D_m can detect successfully s_n and s_m , but an outage occurs in information relaying phase. Accordingly, outage probability of this RF-EH NOMA relaying system is written as

$$\begin{aligned} P_{out} = & \Pr(\gamma_{SD_m}^{s_n} < \gamma_{th}) + \Pr(\gamma_{SD_m}^{s_n} > \gamma_{th}, \gamma_{SD_m}^{s_m} < \gamma_{th}) \\ & + \Pr(\gamma_{SD_m}^{s_n} > \gamma_{th}, \gamma_{SD_m}^{s_m} > \gamma_{th}) \Pr(\gamma_{D_n}^{s_n} < \gamma_{th}). \end{aligned} \quad (19)$$

Notice that because the messages are transmitted in the duration of $(1-\alpha)T/2$, thus γ_{th} is calculated by $\gamma_{th} = 2^{2\Omega/(1-\alpha)} - 1$, where Ω is fixed source transmission rate.

Substituting Eqs. (6), (7), and (13) into Eq. (19), we obtain the following equation:

$$\begin{aligned} P_{out} = & \Pr\left(\frac{b_2 X_2}{b_1 X_2 + 1} < \gamma_{th}\right) + \Pr\left(\frac{b_2 X_2}{b_1 X_2 + 1} > \gamma_{th}, b_1 X_2 < \gamma_{th}\right) \\ & + \Pr\left(\frac{b_2 X_2}{b_1 X_2 + 1} > \gamma_{th}, b_1 X_2 > \gamma_{th}\right) \Pr(c_1 X_1 X_3 < \gamma_{th}) \\ & \times \left[\Pr(b_3 Y_2 < \gamma_{th}) + (1 - \Pr(b_3 Y_2 < \gamma_{th})) \Pr\left(\frac{c_2 Y_1 Y_3}{c_3 Y_3 + 1} < \gamma_{th}\right) \right] \\ = & I_1 + I_2 + I_3 I_4 [I_5 + (1 - I_5) I_6], \end{aligned} \quad (20)$$

where

$$I_1 = \Pr\left(\frac{b_2 X_2}{b_1 X_2 + 1} < \gamma_{th}\right), \quad (21)$$

$$I_2 = \Pr\left(\frac{b_2 X_2}{b_1 X_2 + 1} > \gamma_{th}, b_1 X_2 < \gamma_{th}\right), \quad (22)$$

$$I_3 = \Pr\left(\frac{b_2 X_2}{b_1 X_2 + 1} > \gamma_{th}, b_1 X_2 > \gamma_{th}\right), \quad (23)$$

$$I_4 = \Pr(c_1 X_1 X_3 < \gamma_{th}), \quad (24)$$

$$I_5 = \Pr(b_3 Y_2 < \gamma_{th}), \quad (25)$$

$$I_6 = \Pr\left(\frac{c_2 Y_1 Y_3}{c_3 Y_3 + 1} < \gamma_{th}\right). \quad (26)$$

By the help of Eqs. (14)–(17), we obtain the exact closed-form expressions of I_1 , I_2 , I_3 , I_4 , I_5 , and I_6 , respectively, as follows:

$$I_1 = \begin{cases} 1, & \gamma_{th} > \frac{a_n}{a_m} \\ F_{X_2}\left(\frac{\gamma_{th}}{b_2 - b_1 \gamma_{th}}\right), & \gamma_{th} < \frac{a_n}{a_m} \end{cases} \quad (27)$$

$$= \begin{cases} 1, & \gamma_{th} > \frac{a_n}{a_m} \\ \frac{M!}{(M-m)!(m-1)!} \sum_{k=0}^{m-1} \frac{C_k^{m-1} (-1)^k}{M-m+k+1} \left[1 - e^{-\frac{(M-m+k+1)\gamma_{th}}{\lambda_3(b_2-b_1\gamma_{th})}} \right], & \gamma_{th} < \frac{a_n}{a_m} \end{cases}$$

$$I_2 = \begin{cases} F_{X_2}\left(\frac{\gamma_{th}}{b_1}\right) - F_{X_2}\left(\frac{\gamma_{th}}{b_2 - b_1 \gamma_{th}}\right), & \gamma_{th} < \frac{a_n}{a_m} - 1 \\ 0, & \gamma_{th} > \frac{a_n}{a_m} - 1 \end{cases}$$

$$= \begin{cases} \frac{M!}{(M-m)!(m-1)!} \sum_{k=0}^{m-1} \frac{C_k^{m-1} (-1)^k}{M-m+k+1} \left[e^{-\frac{(M-m+k+1)\gamma_{th}}{\lambda_3(b_2-b_1\gamma_{th})}} - e^{-\frac{(M-m+k+1)\gamma_{th}}{\lambda_3 b_1}} \right], & \gamma_{th} < \frac{a_n}{a_m} - 1 \\ 0, & \gamma_{th} > \frac{a_n}{a_m} - 1 \end{cases} \quad (28)$$

$$I_3 = \begin{cases} 1 - F_{X_2}\left(\frac{\gamma_{th}}{b_1}\right), & \gamma_{th} < \frac{a_n}{a_m} - 1 \\ 1 - F_{X_2}\left(\frac{\gamma_{th}}{b_2 - b_1 \gamma_{th}}\right), & \frac{a_n}{a_m} - 1 < \gamma_{th} < \frac{a_n}{a_m} \\ 0, & \gamma_{th} > \frac{a_n}{a_m} \end{cases}$$

$$= \begin{cases} 1 - \frac{M!}{(M-m)!(m-1)!} \sum_{k=0}^{m-1} \frac{C_k^{m-1} (-1)^k}{M-m+k+1} \left[1 - e^{-\frac{(M-m+k+1)\gamma_{th}}{\lambda_3 b_1}} \right], & \gamma_{th} < \frac{a_n}{a_m} - 1 \\ 1 - \frac{M!}{(M-m)!(m-1)!} \sum_{k=0}^{m-1} \frac{C_k^{m-1} (-1)^k}{M-m+k+1} \left[1 - e^{-\frac{(M-m+k+1)\gamma_{th}}{\lambda_3(b_2-b_1\gamma_{th})}} \right], & \frac{a_n}{a_m} - 1 < \gamma_{th} < \frac{a_n}{a_m} \\ 0, & \gamma_{th} > \frac{a_n}{a_m} \end{cases} \quad (29)$$

$$I_4 = \Pr\left(X_3 < \frac{\gamma_{th}}{c_1 X_1}\right) = \int_0^{\infty} F_{X_3}\left(\frac{\gamma_{th}}{c_1 z}\right) f_{X_1}(z) dz = \int_0^{\infty} \left(1 - e^{-\frac{\gamma_{th}}{\lambda_5 c_1 z}}\right) \frac{1}{\lambda_1} e^{-\frac{z}{\lambda_1}} dz \quad (30)$$

$$= 1 - 2\sqrt{\frac{\gamma_{th}}{\lambda_1 \lambda_5 c_1}} K_1\left(2\sqrt{\frac{\gamma_{th}}{\lambda_1 \lambda_5 c_1}}\right).$$

$$I_5 = 1 - e^{-\frac{\gamma_{th}}{\lambda_4 b_3}}. \quad (31)$$

$$\begin{aligned}
I_6 &= \Pr\left(Y_3 < \frac{c_3\gamma_{th}}{c_2}\right) + \Pr\left(Y_3 < \frac{\gamma_{th}}{c_2 Y_1 - c_3\gamma_{th}}, Y_1 > \frac{c_3\gamma_{th}}{c_2}\right) \\
&= F_{Y_3}\left(\frac{c_3\gamma_{th}}{c_2}\right) + \int_{\frac{c_3\gamma_{th}}{c_2}}^{\infty} F_{Y_3}\left(\frac{\gamma_{th}}{c_2 z - c_3\gamma_{th}}\right) f_{Y_1}(z) dz \\
&= 1 - 2e^{-\frac{c_3\gamma_{th}}{2c_2}} \sqrt{\frac{\gamma_{th}}{\lambda_2 \lambda_6 c_2}} K_1\left(2\sqrt{\frac{\gamma_{th}}{\lambda_2 \lambda_6 c_2}}\right).
\end{aligned} \tag{32}$$

Notice that K_ν is the modified Bessel function of the second kind and ν th order [19].

Substituting Eqs. (27)–(32) into Eq. (20), we obtain the exact closed-form expression of outage probability for this RF-EH NOMA relaying system as follows:

$$P_{out} = \begin{cases} I_1 + I_2 + I_3 I_4 [I_5 + (1 - I_5) I_6], & \gamma_{th} < \frac{a_n}{a_m} - 1. \\ I_1 + I_3 I_4 [I_5 + (1 - I_5) I_6], & \frac{a_n}{a_m} - 1 < \gamma_{th} < \frac{a_n}{a_m}. \\ 1, & \gamma_{th} > \frac{a_n}{a_m}. \end{cases} \tag{33}$$

3.2 Throughput

At this point, we analyze throughput (Φ) at the destination node for delay-limited transmission mode. It is found out by evaluating outage probability at a fixed source transmission rate— Ω bps/Hz. We observe that the source transmit information at the rate of Ω bps/Hz and the effective communication time from the source to the destination in the block time T is $(1-\alpha)T/2$. Therefore, throughput Φ at the destination is defined as follows:

$$\Phi = (1 - P_{out})\Omega \frac{(1 - \alpha)T/2}{T} = \frac{(1 - \alpha)(1 - P_{out})\Omega}{2}. \tag{34}$$

Substituting the result of P_{out} as Eq. (33) in Section 3.1 into Eq. (34), we obtain the exact closed-form expression of throughput for this RF-EH NOMA relaying system.

These derivations are similar to [20]. By using these expressions for programming, we can investigate the behaviors of this considered system, and then we can adjust the inputs to achieve the optimal performance for this network.

4. Numerical results and discussion

In this section, we provide the numerical results according to the system key parameters (i.e., the average transmit SNR γ_0 and γ_S , number of users, time switching ratio, and power allocation coefficients) to clarify the performance of proposed protocol for this considered RF-EH NOMA relaying system. Furthermore, we also provide Monte Carlo simulation results to verify our analytical results. The simulation parameters are shown in **Table 1**.

Figure 5 depicts P_{out} of this considered system versus the average transmit power of power station with different numbers of users M . This figure shows that when we increase the transmit power of power station P , P_{out} of this system

Parameters	System values
Environment	Rayleigh
Number of antennas of each node	1
Fixed rate (Ω)	1 bps/Hz
Number of users (M)	4, 6, 8
Energy conversion efficiency (η)	0.9
Distances (d)	1
Path loss exponent (θ)	2

Table 1.
Simulation parameters.

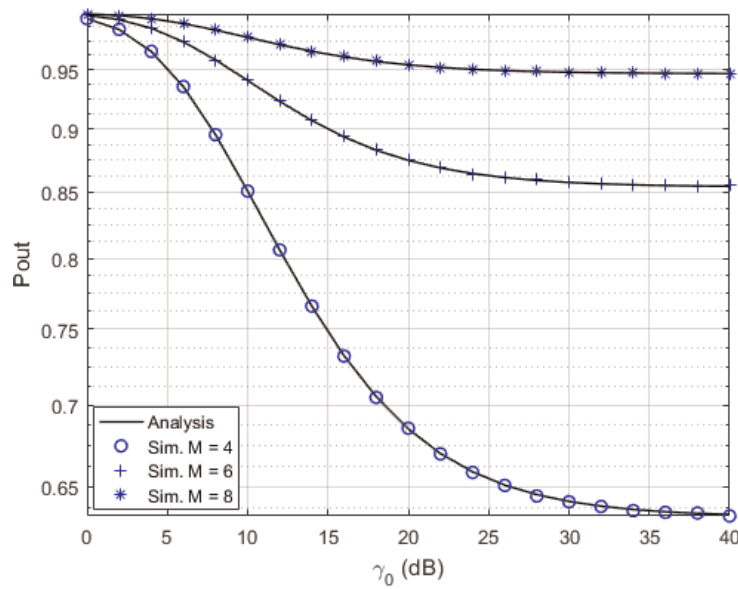


Figure 5.
 P_{out} vs. average transmit SNR of P with different numbers of users M with $\gamma_S = 20$ dB, $a_n = 0.9$, $m = 2$, $n = 3$, $\Omega = 1$ bps/Hz, $\alpha = 0.3$, $\eta = 0.9$, $d_{PDm} = d_{PR} = d_{SDm} = d_{SR} = d_{mn} = d_{RDn} = 1$, $\theta = 2$.

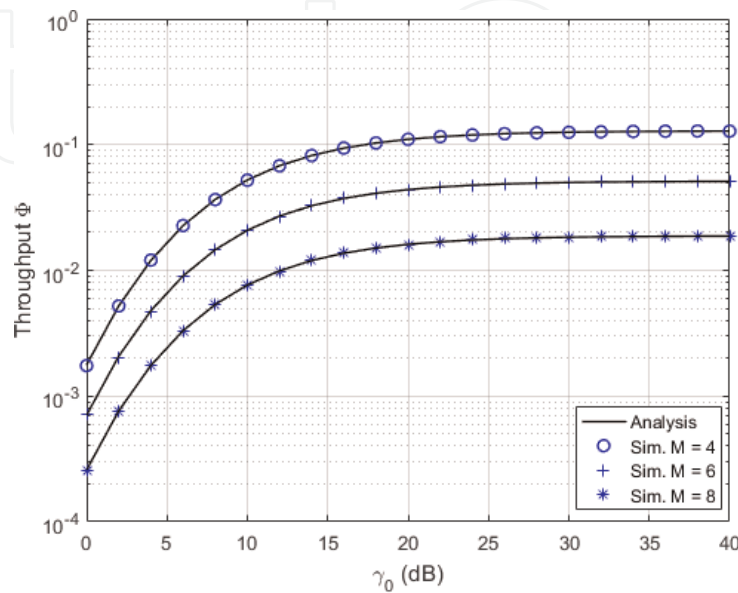


Figure 6.
Throughput Φ vs. average transmit SNR of P with different numbers of users M with $\gamma_S = 20$ dB, $a_n = 0.9$, $m = 2$, $n = 3$, $\Omega = 1$ bps/Hz, $\alpha = 0.3$, $\eta = 0.9$, $d_{PDm} = d_{PR} = d_{SDm} = d_{SR} = d_{mn} = d_{RDn} = 1$, $\theta = 2$.

decreases. Similarly, **Figure 6** shows the variation of throughput with respect to γ_0 for different values of M . This figure also shows that the throughput of this system increases when increasing transmit power of power station P . These mean that we can improve the performance by increasing transmit power to provide more energy to users or reducing the NOMA of users.

Figures 7 and 8 plot the curves of P_{out} and throughput Φ of this system versus time switching ratio for different values of average transmit power of S , respectively. From these figures, we found that when the time switching ratio α is small, α increases, then P_{out} decreases, and Φ increases. This can be explained by that there is more time for the user and relay to harvest energy as α grows. When α continues to increase, P_{out} inversely increases, and Φ decreases. The reason is that there is less time for message transmission phases when α is greater than α^* value. When α is

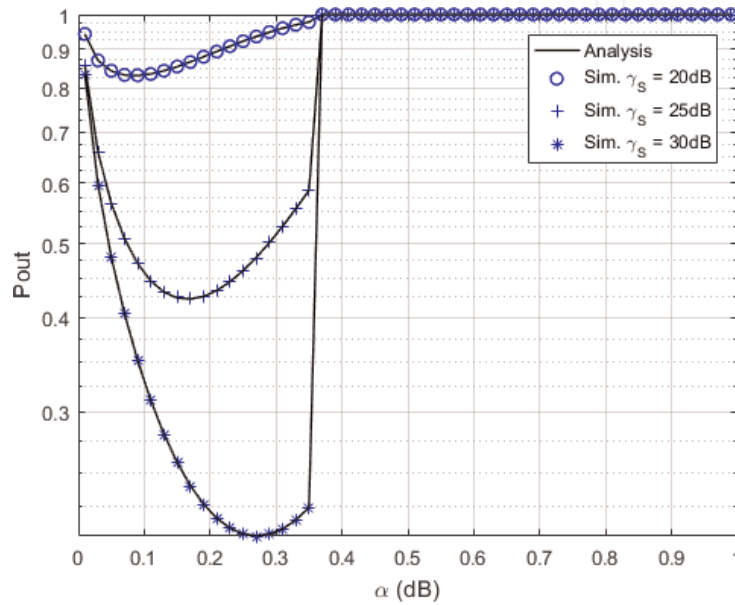


Figure 7.

P_{out} with respect to time switching ratio for different values of average transmit SNR of S with $\gamma_0 = 20$ dB, $M = 8$, $m = 2$, $n = 3$, $\Omega = 1$ bps/Hz, $a_n = 0.9$, $\eta = 0.9$, $d_{PDm} = d_{PR} = d_{SDm} = d_{SR} = d_{mn} = d_{RDn} = 1$, $\theta = 2$.

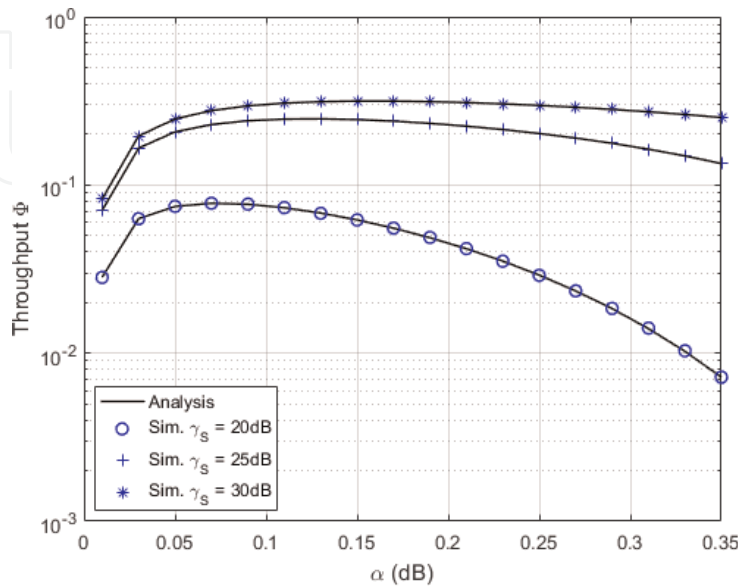


Figure 8.

Throughput Φ with respect to time switching ratio for different values of average transmit SNR of S with $\gamma_0 = 20$ dB, $M = 8$, $m = 2$, $n = 3$, $\Omega = 1$ bps/Hz, $a_n = 0.9$, $\eta = 0.9$, $d_{PDm} = d_{PR} = d_{SDm} = d_{SR} = d_{mn} = d_{RDn} = 1$, $\theta = 2$.

greater than $1 - 2\Omega/\log_2(a_n/a_m + 1)$, then P_{out} reaches 1. From this analysis, there exists a specific value of α^* that leads P_{out} to obtain the lowest value and leads Φ to reach the highest value. Obviously, we can select the best time switching ratio α to achieve the optimal performance of this system. From these figures, we also found that the performance of this system can be improved by increasing the transmit power of source S.

Figures 9 and 10 show the variation of P_{out} and throughput Φ with respect to power allocation coefficient a_n for different values of average transmit SNR of S, respectively. From these figures, we can see that when $a_n \rightarrow 1$, the performance of this system degrades. Due to the constrain of γ_{th} (i.e., $\gamma_{th} = 2^{2\Omega/(1-\alpha)} - 1 < a_n/a_m$), by the given value of R and α , the P_{out} reaches 1 when $a_n/a_m < 2^{2\Omega/(1-\alpha)} - 1$. According to these figures, the performance can be improved when $a_n \rightarrow 0.89$ for $\Omega = 1$ bps/Hz,

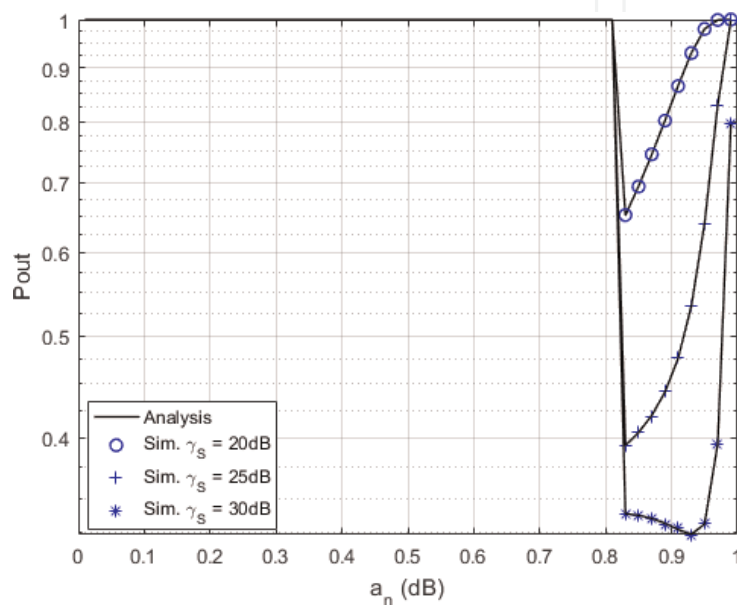


Figure 9.

P_{out} with respect to power allocation coefficient a_n for different values of average transmit SNR of S with $\gamma_o = 20$ dB, $M = 8$, $m = 2$, $n = 3$, $\Omega = 1$ bps/Hz, $\alpha = 0.1$, $\eta = 0.9$, $d_{PDm} = d_{PR} = d_{SDm} = d_{SR} = d_{mn} = d_{RDn} = 1$, $\theta = 2$.

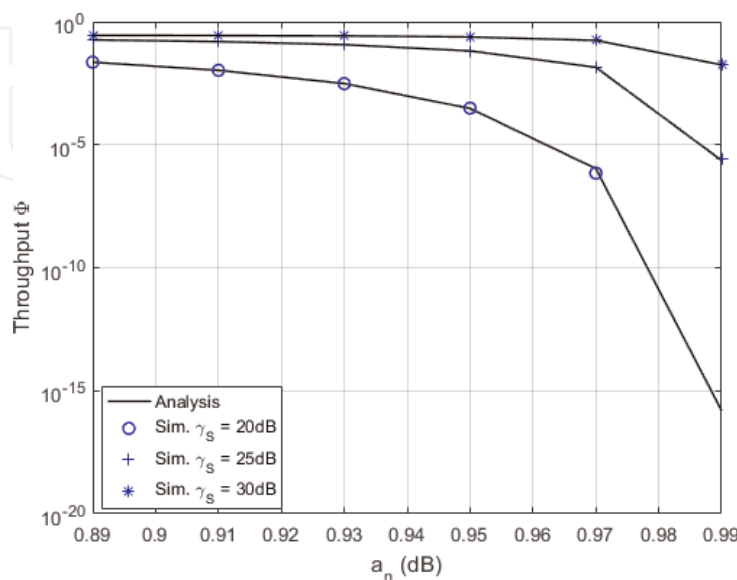


Figure 10.

Throughput Φ with respect to power allocation coefficient for different values of average transmit SNR of S with $\gamma_o = 20$ dB, $M = 8$, $m = 2$, $n = 3$, $\Omega = 1$ bps/Hz, $\alpha = 0.1$, $\eta = 0.9$, $d_{PDm} = d_{PR} = d_{SDm} = d_{SR} = d_{mn} = d_{RDn} = 1$, $\theta = 2$.

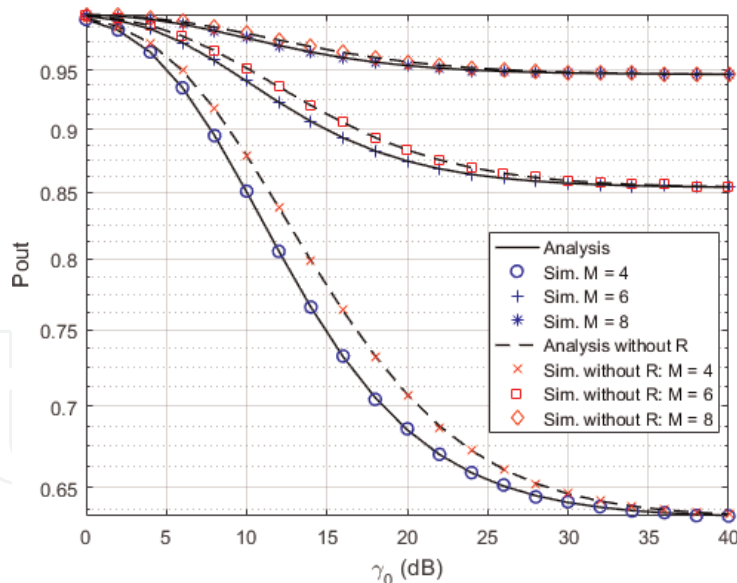


Figure 11.

P_{out} with and without relay vs. average transmit SNR of P with different numbers of users M with $\gamma_S = 20$ dB, $a_n = 0.9$, $m = 2$, $n = 3$, $\Omega = 1$ bps/Hz, $\alpha = 0.3$, $\eta = 0.9$, $d_{PDm} = d_{PR} = d_{SDm} = d_{SR} = d_{mn} = d_{RDn} = 1$, $\theta = 2$.

$\alpha = 0.1$. In order to improve the performance of this system, we can allocate more transmit power for the worse user's message (i.e., s_n). However, at that time the power which leaves for the better user's message (i.e., s_m) will be smaller, and it should satisfy $a_n/a_m > 2^{2\Omega/(1-\alpha)} - 1$.

In addition, **Figure 11** plots the curves of P_{out} with and without relay versus average transmit SNR of power station P with different numbers of users M . In this figure, we can observe that P_{out} of relaying scheme is lower than P_{out} without relaying. In other words, this result confirms that relaying method can improve the performance of this considered system.

Finally, we can observe from the above figures that the analysis and simulation results are good matching. This confirms the correctness of our analysis.

5. Conclusions

In this chapter, we have presented the performance analysis of downlink RF-EH NOMA relaying network with triple-phase harvest-transmit-forward transmission protocol in terms of outage probability and throughput. The exact closed-form expressions of outage probability and throughput for this proposed system have been derived. We have found that the performance of this considered system is enhanced by applying relaying technique or increasing the transmit power for energy harvesting and/or increasing the transmit power for information transmission. Moreover, the existence of best time switching ratio is proven to achieve the optimal performance of this system. We will solve the best time switching ratio searching problem in the future work.

IntechOpen

IntechOpen

Author details

Dac-Binh Ha^{1*} and Jai P. Agrawal²

1 Duy Tan University, Da Nang, Vietnam

2 Purdue University Northwest, Hammond, IN, USA

*Address all correspondence to: hadacbinh@duytan.edu.vn

IntechOpen

© 2019 The Author(s). Licensee IntechOpen. This chapter is distributed under the terms of the Creative Commons Attribution License (<http://creativecommons.org/licenses/by/3.0>), which permits unrestricted use, distribution, and reproduction in any medium, provided the original work is properly cited. 

References

- [1] Bi S, Zeng Y, Zhang R. Wireless powered communication networks: An overview. *IEEE Wireless Communications*. 2016;**23**(2):10-18. DOI: 10.1109/MWC.2016.7462480
- [2] Adu-Manu KS, Adam N, Tapparello C, Ayatollahi H, Heinzelman W. Energy-harvesting wireless sensor networks (EH-WSNs): A review. *ACM Transactions on Sensor Networks*. 2018;**14**(2):1-50. DOI: 10.1145/3183338
- [3] Sing K, Moh S. Energy harvesting in wireless sensor networks: Techniques and issues. *International Journal of Control and Automation*. 2017;**10**(6): 71-84. DOI: 10.14257/ijca.2017.10.6.08 [Accessed: 2019-05-15]
- [4] Cheng J, Chen W, Tao F, Lin C-L. Industrial IoT in 5G environment towards smart manufacturing. *Journal of Industrial Information Integration*. 2018;**10**:10-19. DOI: 10.1016/j.jii.2018.04.001. [Accessed: 2019-05-18]
- [5] Akpakwu GA, Silva BJ, Hancke GP, Abu-Mahfouz AM. A survey on 5G networks for the internet of things: Communication technologies and challenges. *IEEE Access*. 2018;**6**: 3619-3647. DOI: 10.1109/ACCESS.2017.2779844
- [6] Guanyao D, Xiong K, Qiu Z. Outage analysis of cooperative transmission with energy harvesting relay: Time switching versus power splitting. *Mathematical Problems in Engineering*. 2015;**2015**:1-9. DOI: 10.1155/2015/598290. [Accessed: 2019-03-18]
- [7] Chakrabarti A, Sabharwal A, Aazhang B. *Cooperative Communications: Fundamental Limits and Practical Implementation*. Springer Publishers; 2006. Available from: <https://scholarship.rice.edu/handle/1911/19781>. [Accessed: 2019-09-14]
- [8] Nasir AA, Zhou X, Durrani S, Kennedy RA. Relaying protocols for wireless energy harvesting and information processing. *IEEE Transactions on Wireless Communications*. 2015;**12**(7): 3622-3636. DOI: 10.1109/TWC.2013.062413.122042
- [9] Ha D-B, Tran D-D, Tran-Ha V, Hong E-K. Performance of amplify-and-forward relaying with wireless power transfer over dissimilar channels. *Elektronika ir Elektrotechnika Journal*. 2015;**21**(5):90-95. DOI: 10.5755/j01.eee.21.5.13331
- [10] Cvetkovic A, Blagojevic V, Ivaniš P. Performance analysis of nonlinear energy-harvesting DF relay system in interference-limited Nakagami- m fading environment. *ETRI Journal*. 2017;**39**(6):803-812. DOI: 10.4218/etrij.2017-0096. [Accessed: 2019-03-18]
- [11] Islam SMR, Avazov N, Dobre OA, Kwak K-s. Power-domain non-orthogonal multiple access (NOMA) in 5G systems: Potentials and challenges. *IEEE Communication Surveys and Tutorials*. 2017;**19**(2):721-742. DOI: 10.1109/COMST.2016.2621116
- [12] Ha D-B, Nguyen SQ. Outage performance of energy harvesting DF relaying NOMA networks. *Mobile Networks and Applications*. 2018;**23**(6): 1572-1585. DOI: 10.1007/s11036-017-0922-x. [Accessed: 2019-03-18]
- [13] Tran D-D, Ha D-B, Vo VN, So-In C, et al. Performance analysis of DF/AF cooperative MISO wireless sensor networks with NOMA and SWIPT over Nakagami- m fading. *IEEE Access*. 2018;**6**:56142-56161. DOI: 10.1109/ACCESS.2018.2872935
- [14] Tran DD, Tran HV, Ha DB, Kaddoum G. Cooperation in NOMA networks under limited user-to-user

communications: Solution and analysis.
In: Proceedings of 2018 IEEE Wireless Communications and Networking Conference (WCNC'18); Barcelona, Spain: 15-18 April 2018. 2018

[15] Ha D-B, Nguyen SQ, Nguyen HT. Cooperative cognitive non-orthogonal multiple access under unreliable backhaul connections. *Mobile Networks and Applications*. 2019;24(2):596-617. DOI: 10.1007/s11036-018-1161-5. [Accessed: 2019-03-18]

[16] Tran D-D, Tran H-V, Ha D-B, Kaddoum G. Secure transmit antenna selection protocol for MIMO NOMA networks over Nakagami-m channels. *IEEE Systems Journal (Early Access)*. 2019:1-12. DOI: 10.1109/JSYST.2019.2900090

[17] Ding Z, Peng M, Poor HV. Cooperative non-orthogonal multiple access in 5G systems. *IEEE Communications Letters*. 2015;19(8):1462-1465. DOI: 10.1109/LCOMM.2015.2441064

[18] Men J, Ge J. Performance analysis of non-orthogonal multiple access in downlink cooperative network. *IET Communications*. 2015;9(18):2267-2273. DOI: 10.1049/iet-com.2015.0203

[19] Gradshteyn IS, Ryzhik IM. *Table of Integrals, Series and Products*. 7th ed. Academic Press; 2007. Available from: <https://www.sciencedirect.com/book/9780123849335/table-of-integrals-series-and-products>

[20] Ha DH, Ha DB, Voznak M. On secure cooperative non-orthogonal multiple access network with RF power transfer. In: Proceedings of 2019—5th EAI International Conference on Industrial Networks and Intelligent Systems; Hochiminh City, Vietnam; 19 August. 2019